

Supplementary Material

Synthesis, Structure and Magnetic Behaviour of the Manganese(II) Selenide/Selenolate Cluster Complexes $[\text{Mn}_{32}\text{Se}_{14}(\text{SePh})_{36}(\text{PnPr}_3)_4]$ and $[\text{Na}(\text{benzene-15-Crown-5})(\text{C}_4\text{H}_8\text{O})_2]_2[\text{Mn}_8\text{Se}(\text{SePh})_{16}]$

Andreas Eichhöfer, Paul T. Wood, Raghavan N. Viswanath, Richard A. Mole

Experimental

Synthesis

Standard Schlenk techniques were employed throughout the syntheses using a double manifold vacuum line with high purity dry nitrogen. The solvents THF and diethylether were dried over sodium-benzophenone and toluene over LiAlH₄, and distilled under nitrogen. Mn(SePh)₂,¹ PhSeSiMe₃^[2] and Se(SiMe₃)₂^[3] were prepared according to literature procedures.

Crystallography

Crystals suitable for single X-ray diffraction were taken directly from the reaction solution of the compound and then selected in perfluoroalkylether oil. Single-crystal X-ray diffraction data of **1** were collected using synchrotron radiation ($\lambda = 0.80 \text{ \AA}$) on a STOE IPDS II (Imaging Plate Diffraction System) at the ANKA synchrotron source in Karlsruhe. Single-crystal X-ray diffraction data of **2** were collected using graphite-monochromatized MoK α radiation ($\lambda = 0.71073 \text{ \AA}$) on a STOE IPDS II (Imaging Plate Diffraction System) equipped with a Schneider rotating anode. The structures were solved with the direct methods program SHELXS^[4] of the SHELXTL PC suite programs, and were refined with the use of the full-matrix least-squares program SHELXL.^[4] Molecular diagrams were prepared using SCHAKAL 97^[5].

In **1** all Mn, Se, P and C atoms with the exception of the C atoms of the *n*-propyl groups of the phosphine ligands (C19 – C21) were refined with anisotropic displacement parameters whilst H atoms were calculated in fixed positions. The C atoms of the *n*-propyl groups of the phosphine ligands (C19 – C21) show due to disorder, which could not be modelled, large Ueq values. The difference Fourier map indicated areas of disordered solvent molecules which were located by the program ‘Squeeze’ as part of the PLATON^[6] program package to give a total potential solvent area of $4361 \cdot 10^6 \text{ pm}^3$. The dataset was corrected for this theoretically possible additional amount of electron density. In **2** all Mn, Se and C atoms of the cluster anion $[\text{Mn}_8\text{Se}(\text{SePh})_{16}]^{2-}$ were refined with anisotropic displacement parameters with the

exception of C35 and C36 which were modelled isotropically in two splitted positions. The Na, C and O atoms of the two $[\text{Na}(\text{benzene-15-Crown-5})(\text{C}_4\text{H}_8\text{O})_2]^+$ counterions were calculated with isotropic displacement parameters. Due to disorder some of the bond distances in one of the counterions (Na2) have been fixed and C130 has been treated with a split refinement in order to give a reasonable structural model. In addition to one localized thf solvent molecule the difference fourier map indicated areas of further disordered solvent molecules which could not be identified or refined properly. CCDC-612695 (**1**), and -612696 (**2**) contain the supplementary crystallographic data for this paper.

X-ray powder diffraction patterns (XRD) were measured on a STOE STADI P diffractometer (Cu-K α 1 radiation, Germanium monochromator, Debye-Scherrer geometry) in sealed glass capillaries. A theoretical powder diffraction pattern for **1** was calculated on the basis of the atom coordinates obtained from single crystal X-ray analysis by using the program package STOE WinXPOW.^[7]

Physical Measurements

UV-Vis absorption spectra of cluster molecules in solution were measured on a Varian Cary 500 spectrophotometer in quartz cuvettes. Solid state reflection spectra were measured as micron sized crystalline powders between quartz plates with a Labsphere integrating sphere. Zero-Field-Cooled temperature dependent susceptibilities were recorded for **1** and **2** in RSO mode using a MPMS-5S (Quantum Design) SQUID magnetometer over a temperature range of 5 to 300 K in a homogeneous 100 G external magnetic field. Field dependent susceptibilities were recorded on a Quantum Design PPMS extraction magnetometer, recording the response to the vertical movement 10 m/s of the sample through the detection coils, under dry helium environment. The samples were contained in high-precision quartz glass sample holders owing to the high degree of moisture sensitivity of the compounds. The data were corrected for the sample holder and for diamagnetism using Pascal's constants.⁸

Figures

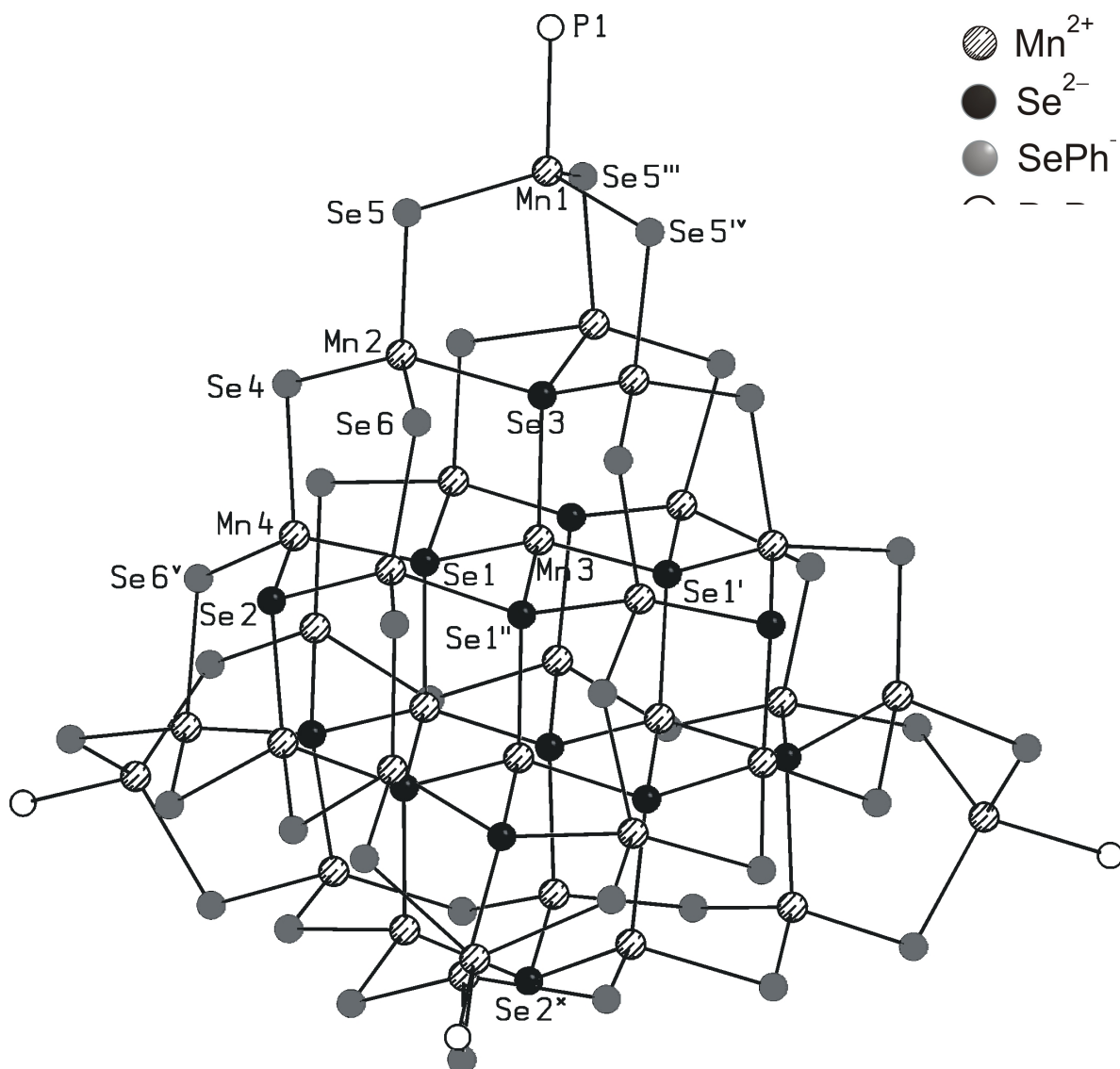


Figure 1. The $\text{Mn}_{32}\text{Se}_{50}\text{P}_4$ cluster core as a section of the molecular structure of $[\text{Mn}_{32}\text{Se}_{14}(\text{SePh})_{36}(\text{PnPr}_3)_4]$ (**1**). Symmetry transformation for generation of equivalent atoms: ^I $z+1, -x+1, -y$; ^{II} $y+1, z, x-1$; ^{III} $-z+1, x-1, -y$; ^{IV} $y+1, -z, -x+1$; ^V $z+1, x-1, y$; ^X $-x+2, -y, z$.

Selected bond length [pm] and angles [°]: $\text{Mn}(1)-\text{P}(1)$ 252.2(9), $\text{Mn}(1)-\text{Se}(5)$ 256.0(2), $\text{Mn}(2)-\text{Se}(3)$ 257.1(2), $\text{Mn}(2)-\text{Se}(5)$ 257.8(2), $\text{Mn}(2)-\text{Se}(6)$ 255.8(2), $\text{Mn}(2)-\text{Se}(4)$ 255.5(2), $\text{Mn}(3)-\text{Se}(1)$ 253.3(1), $\text{Mn}(3)-\text{Se}(3)$ 254.6(3), $\text{Mn}(4)-\text{Se}(1)$ 255.3(2), $\text{Mn}(4)-\text{Se}(2)$ 249.4(2), $\text{Mn}(4)-\text{Se}(4)$ 260.5(2), $\text{Mn}(4)-\text{Se}(6)$ ^V 258.7(2). $\text{P}(1)-\text{Mn}(1)-\text{Se}(5)$ 104.36(7) $\text{P}(1)-\text{Mn}(1)-\text{Se}(5)^{\text{III}}$ 104.36(7), $\text{Se}(5)-\text{Mn}(1)-\text{Se}(5)^{\text{III}}$ 114.06(6), $\text{P}(1)-\text{Mn}(1)-\text{Se}(5)^{\text{IV}}$ 104.36(7), $\text{Se}(5)-\text{Mn}(1)-\text{Se}(5)^{\text{IV}}$ 114.06(6), $\text{Se}(5)^{\text{III}}-\text{Mn}(1)-\text{Se}(5)^{\text{IV}}$ 114.06(6), $\text{Se}(4)-\text{Mn}(2)-\text{Se}(6)$ 122.31(8), $\text{Se}(4)-\text{Mn}(2)-\text{Se}(3)$ 122.41(8), $\text{Se}(6)-\text{Mn}(2)-\text{Se}(3)$ 88.56(6), $\text{Se}(4)-\text{Mn}(2)-\text{Se}(5)$ 114.19(7), $\text{Se}(6)-\text{Mn}(2)-\text{Se}(5)$ 97.72(7), $\text{Se}(3)-\text{Mn}(2)-\text{Se}(5)$ 106.73(8), $\text{Se}(1)^{\text{I}}-\text{Mn}(3)-\text{Se}(1)$ 111.23(6), $\text{Se}(1)^{\text{I}}-\text{Mn}(3)-\text{Se}(1)^{\text{II}}$ 111.23(6), $\text{Se}(1)-\text{Mn}(3)-\text{Se}(1)^{\text{II}}$ 111.23(6), $\text{Se}(1)^{\text{I}}-\text{Mn}(3)-\text{Se}(3)$ 107.65(6), $\text{Se}(1)-\text{Mn}(3)-\text{Se}(3)$ 107.65(6), $\text{Se}(1)^{\text{II}}-\text{Mn}(3)-\text{Se}(3)$ 107.65(6), $\text{Se}(2)-\text{Mn}(4)-\text{Se}(1)$ 117.15(8), $\text{Se}(2)-\text{Mn}(4)-\text{Se}(6)$ ^V 113.89(7), $\text{Se}(1)-\text{Mn}(4)-\text{Se}(6)$ ^V 100.39(7), $\text{Se}(2)-\text{Mn}(4)-\text{Se}(4)$ 116.41(8), $\text{Se}(1)-\text{Mn}(4)-\text{Se}(4)$ 102.74(7).

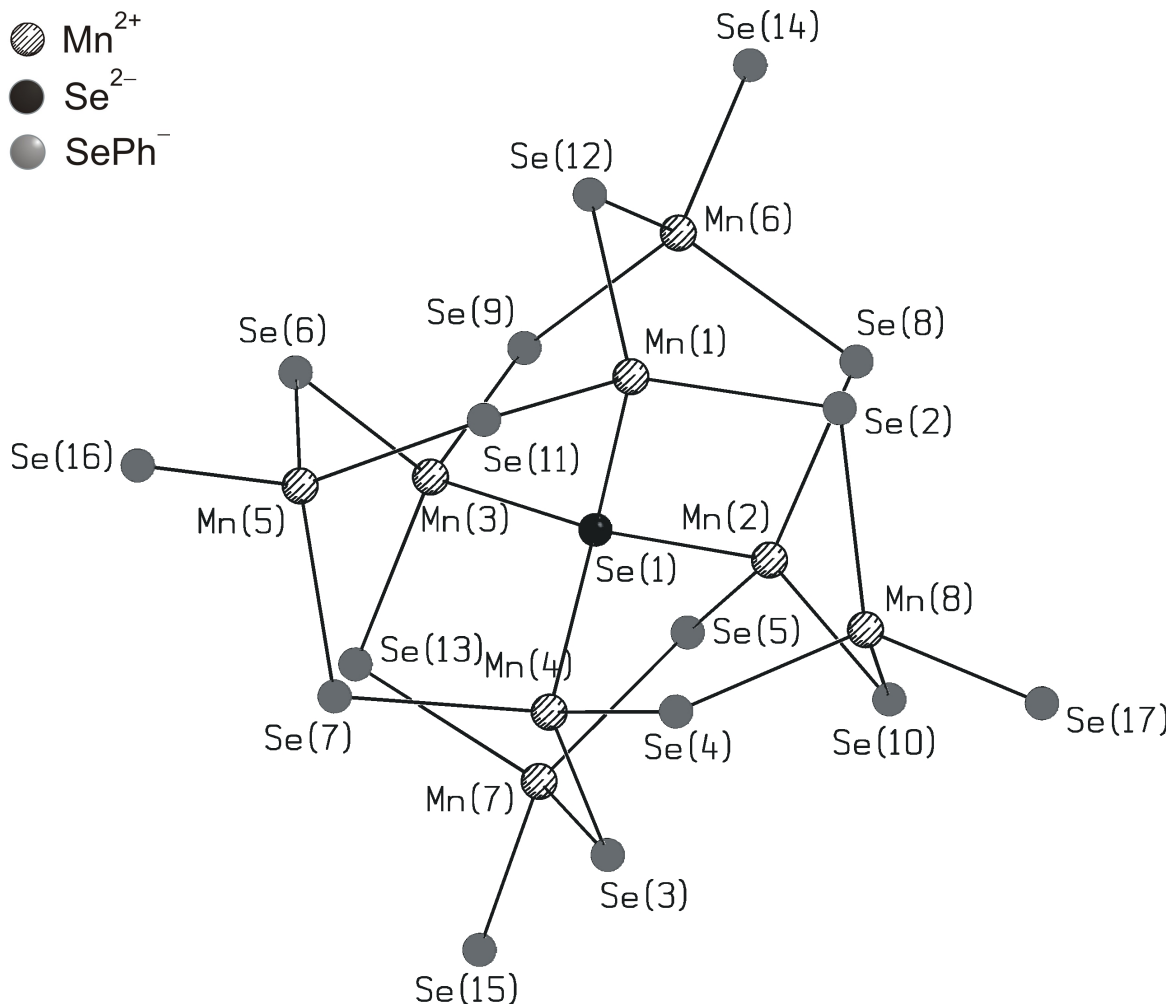


Figure 2. The $\text{Mn}_8\text{Se}_{17}$ cluster core as a section of the molecular structure of $[\text{Na}(\text{benzene-15-Crown-5})(\text{C}_4\text{H}_8\text{O})_2]_2[\text{Mn}_8\text{Se}(\text{SePh})_{16}]$ (**2**).

Selected bond length [pm] and angles [$^\circ$]: Se(1)–Mn(3) 252.5(2), Se(1)–Mn(1) 252.6(2), Se(1)–Mn(4) 252.8(2), Se(1)–Mn(2) 253.4(2), Se(2)–Mn(1) 255.3(2), Se(2)–Mn(8) 262.0(2), Se(3)–Mn(4) 254.4(2), Se(3)–Mn(7) 259.3(2), Se(4)–Mn(4) 256.5(2), Se(4)–Mn(8) 260.2(2), Se(5)–Mn(2) 256.9(2), Se(5)–Mn(7) 259.9(2), Se(6)–Mn(3) 256.0(2), Se(6)–Mn(5) 259.4(2), Se(7)–Mn(4) 256.0(2), Se(7)–Mn(5) 260.6(2), Se(8)–Mn(2) 255.2(2), Se(8)–Mn(6) 260.6(2), Se(9)–Mn(3) 254.9(2), Se(9)–Mn(6) 260.5(2), Se(10)–Mn(2) 255.8(2), Se(10)–Mn(8) 260.1(2), Se(11)–Mn(1) 256.1(2), Se(11)–Mn(5) 260.6(2), Se(12)–Mn(1) 255.7(2), Se(12)–Mn(6) 259.8(2), Se(13)–Mn(3) 254.9(2), Se(13)–Mn(7) 260.1(2), Se(14)–Mn(6) 248.8(2), Se(15)–Mn(7) 247.8(2), Se(16)–Mn(5) 250.1(2), Se(17)–Mn(8) 250.6(2). Se(1)–Mn(1)–Se(2) 102.42(5), Se(1)–Mn(1)–Se(12) 102.43(5), Se(2)–Mn(1)–Se(12) 115.10(6), Se(1)–Mn(1)–Se(11) 103.55(5), Se(2)–Mn(1)–Se(11) 116.79(6), Se(12)–Mn(1)–Se(11) 113.81(6), Se(1)–Mn(2)–Se(8) 103.00(6), Se(1)–Mn(2)–Se(10) 103.14(6), Se(8)–Mn(2)–Se(10) 113.22(6), Se(1)–Mn(2)–Se(5) 103.81(6), Se(8)–Mn(2)–Se(5) 114.15(6), Se(10)–Mn(2)–Se(5) 117.19(6), Se(1)–Mn(3)–Se(13) 105.56(6), Se(1)–Mn(3)–Se(9) 102.49(6), Se(13)–Mn(3)–Se(9) 114.79(6), Se(1)–Mn(3)–Se(6) 103.06(6), Se(13)–Mn(3)–Se(6) 115.17(7), Se(9)–Mn(3)–Se(6) 113.72(6), Se(1)–Mn(4)–Se(3) 99.33(5), Se(1)–Mn(4)–Se(7) 102.95(6), Se(3)–Mn(4)–Se(7) 114.83(6), Se(1)–Mn(4)–Se(4) 105.47(5), Se(3)–Mn(4)–Se(4) 114.58(6), Se(7)–Mn(4)–Se(4) 116.69(6), Se(16)–Mn(5)–Se(6) 118.89(7), Se(16)–Mn(5)–Se(7) 112.45(7), Se(6)–Mn(5)–Se(7) 105.14(6), Se(16)–Mn(5)–Se(11) 107.56(6), Se(6)–Mn(5)–Se(11) 105.61(6), Se(7)–Mn(5)–Se(11) 106.38(6), Se(14)–Mn(6)–Se(12) 116.89(7), Se(14)–Mn(6)–

Se(9) 113.30(7), Se(12)–Mn(6)–Se(9) 105.13(7), Se(14)–Mn(6)–Se(8) 104.65(8), Se(12)–Mn(6)–Se(8) 107.76(6), Se(9)–Mn(6)–Se(8) 108.84(6), Se(15)–Mn(7)–Se(3) 107.13(7), Se(15)–Mn(7)–Se(5) 124.36(7), Se(3)–Mn(7)–Se(5) 106.94(6), Se(15)–Mn(7)–Se(13) 106.23(7), Se(3)–Mn(7)–Se(13) 106.23(6), Se(5)–Mn(7)–Se(13) 104.73(6), Se(17)–Mn(8)–Se(10) 102.83(6), Se(17)–Mn(8)–Se(4) 114.77(6), Se(10)–Mn(8)–Se(4) 108.37(6), Se(17)–Mn(8)–Se(2) 116.58(6), Se(10)–Mn(8)–Se(2) 108.03(6), Se(4)–Mn(8)–Se(2) 105.87(6).

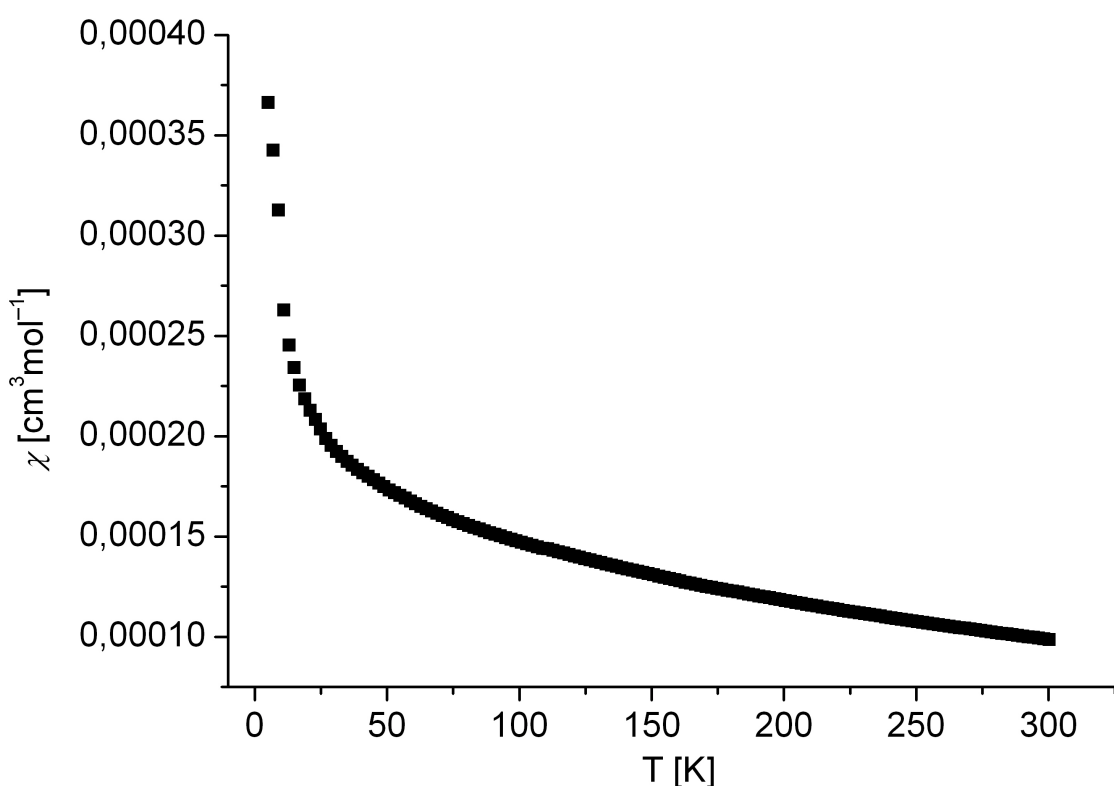


Figure 3. Temperature dependence of the susceptibility of **1**.

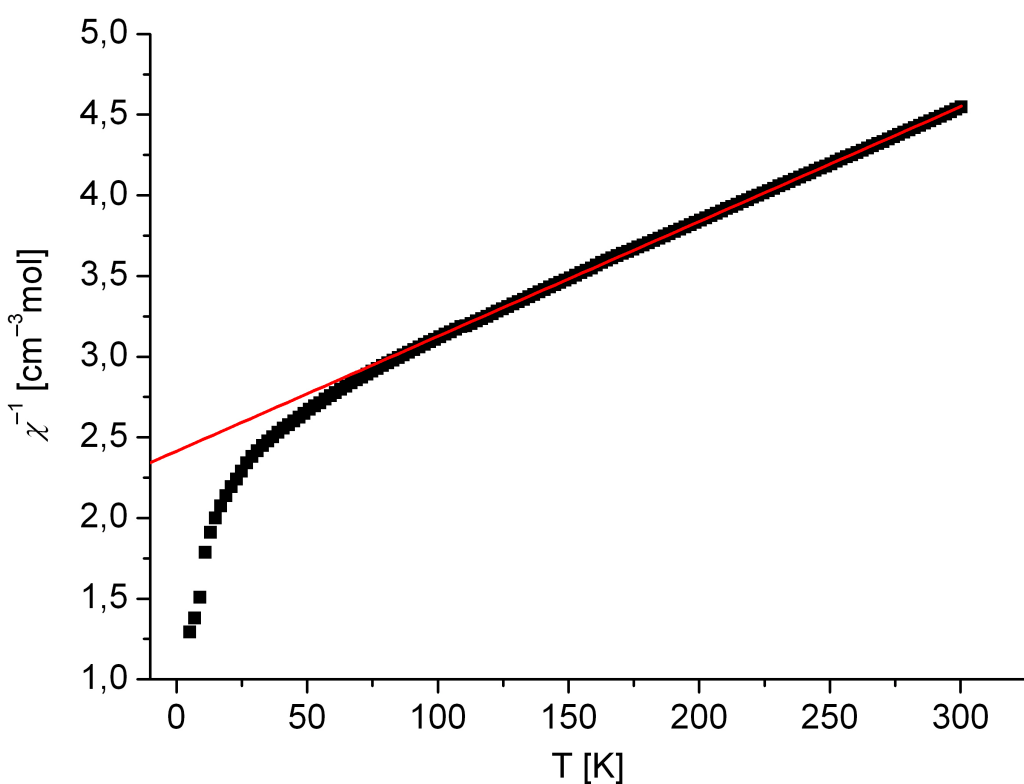


Figure 4. Temperature dependence of the inverse susceptibility of **1** with the fit for $T > 100$ K to the Curie-Weiss law.

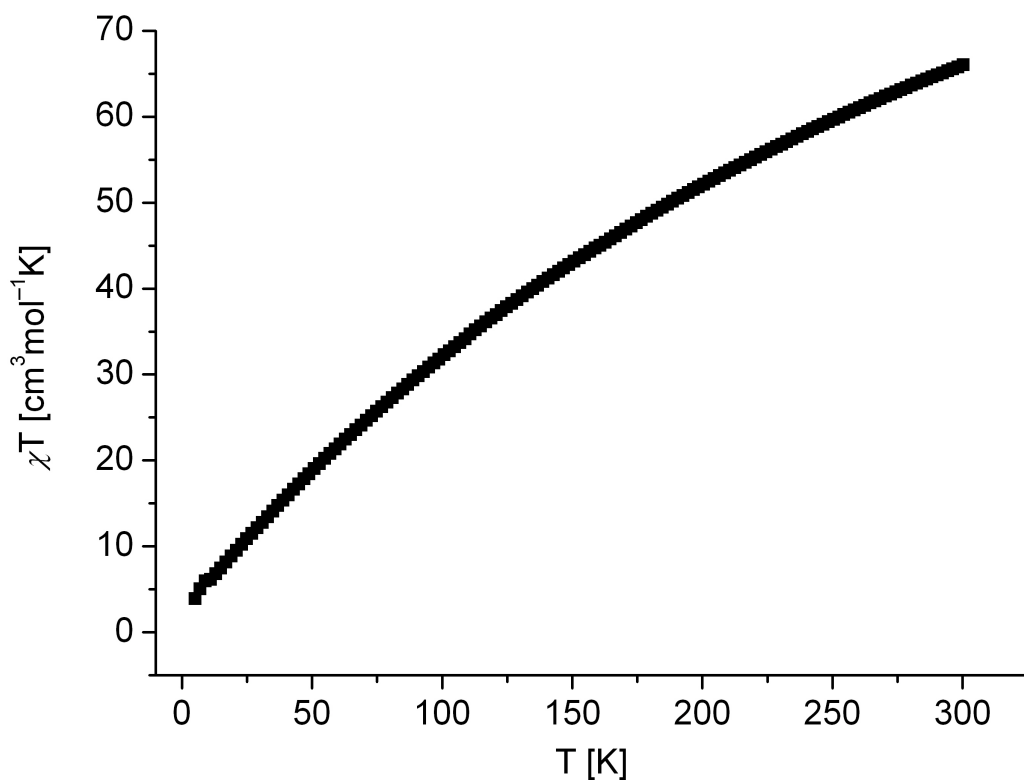


Figure 5. Graph of χT versus T for **1**.

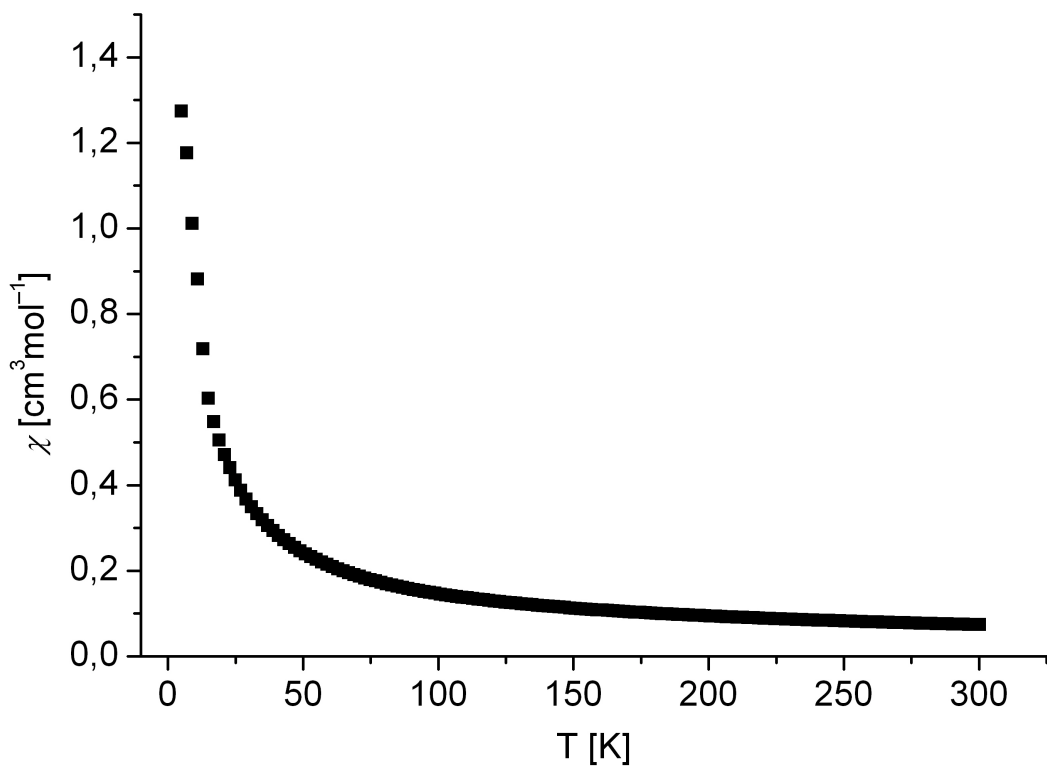


Figure 6. Temperature dependence of the susceptibility of **2**.

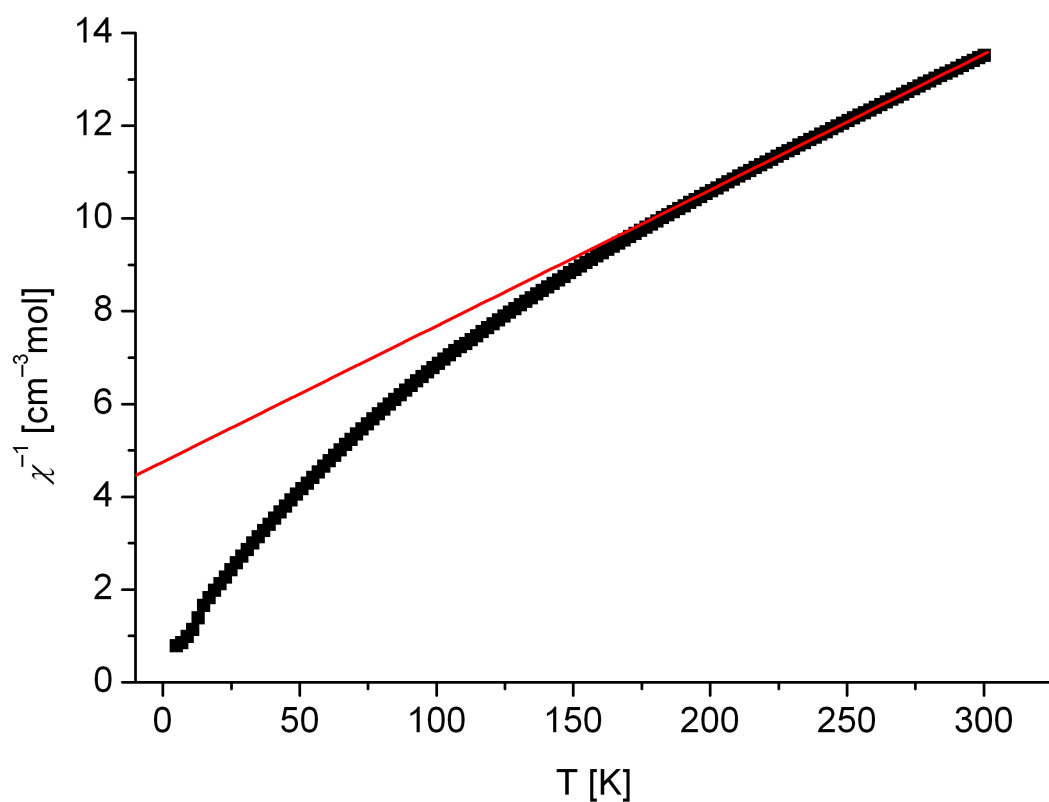


Figure 7. Temperature dependence of the inverse susceptibility of **2** with the fit for $T > 200$ K to the Curie-Weiss law.

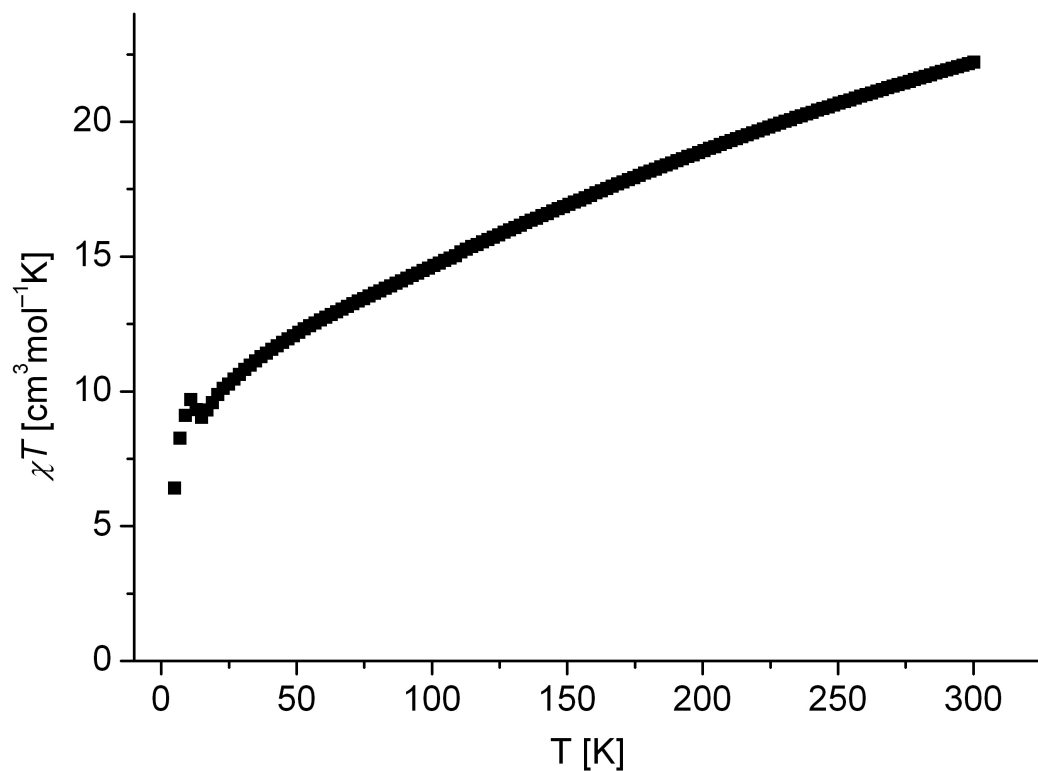


Figure 8. Graph of χT versus T for **2**.

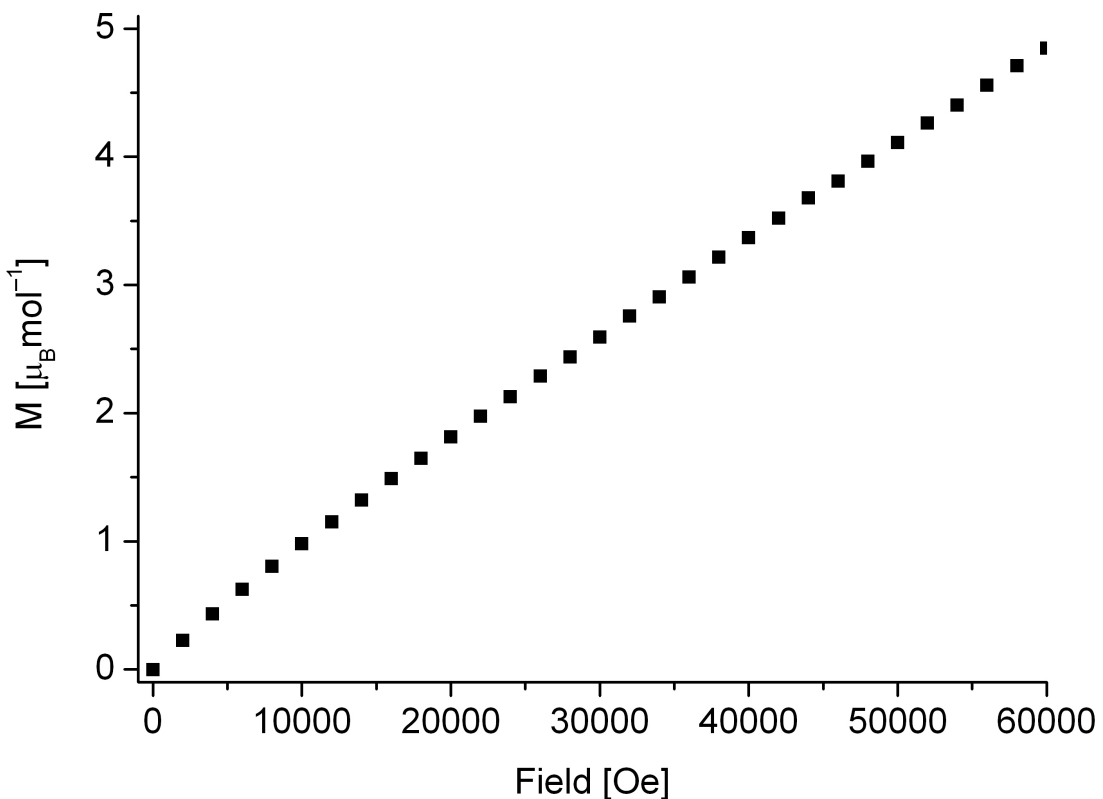


Figure 9. Magnetisation *vs* field for **1** at 2K.

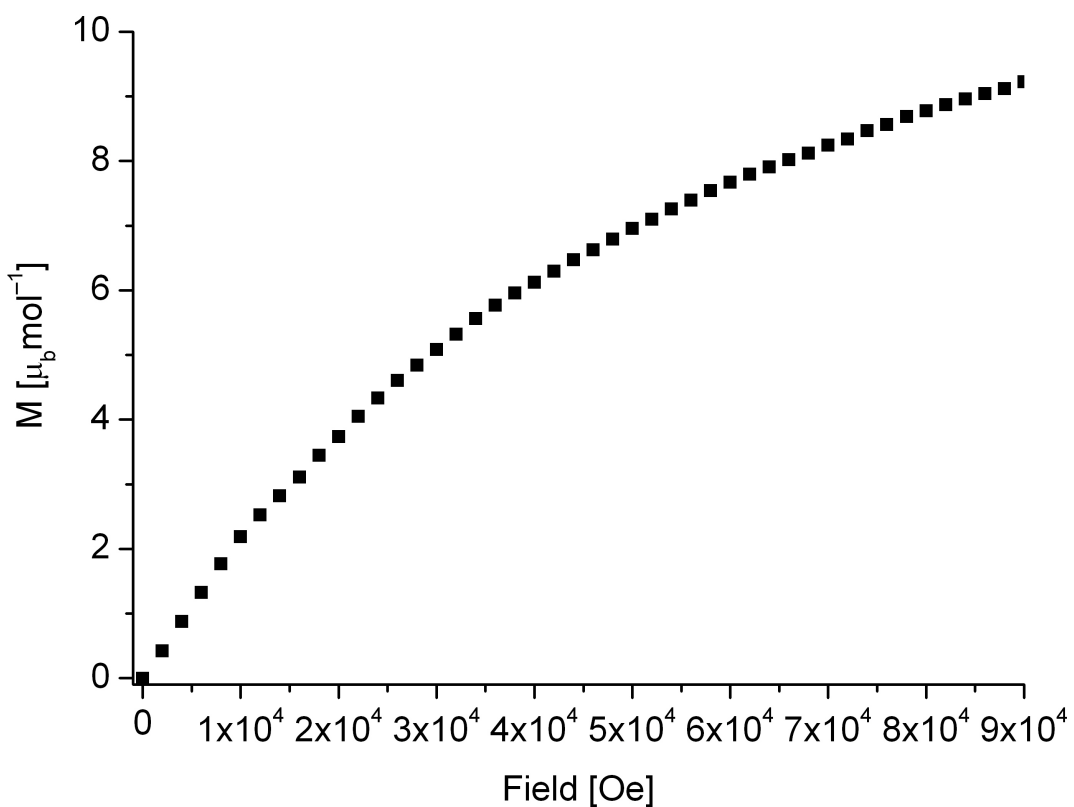


Figure 10. Magnetisation *vs* field for **2** at 2K.

Table 1: Selected interatomic Se–Mn bond distances in $[\text{Mn}_{32}\text{Se}_{14}(\text{SePh})_{36}(\text{PnPr}_3)_4]$ (**1**) and $[\text{Na}(\text{benzene-15-Crown-5})(\text{C}_4\text{H}_8\text{O})_2]_2[\text{Mn}_8\text{Se}(\text{SePh})_{16}]$ (**2**).

Compound	Bonding atoms	Range of distances [pm]	No. of bonds	Average bond distance [pm]
1	$\mu_3\text{-Se-Mn}$	Se(2)–Mn(4): 249.4(2)	12	249.4
	$\mu_4\text{-Se-Mn}$	Se(1)–Mn(3): 253.3(1) – Se(3)–Mn(2): 257.1(2)	40	255.2
	$\mu_2\text{-PhSe-Mn}$	Se(4)–Mn(2): 255.5(2) – Se(4)–Mn(4): 260.5(2)	72	256.9
2	$\mu_1\text{-PhSe-Mn}$	Se(14)–Mn(6): 248.8(2) – Se(17)–Mn(8): 250.6(2)	4	249.4
	$\mu_2\text{-PhSe-Mn}$	Se(8)–Mn(2): 255.2(2) – Se(2)–Mn(8): 262.2(2)	24	257.9
	$\mu_4\text{-Se-Mn}$	Se(1)–Mn(3): 252.5(2) – Se(1)–Mn(2): 253.4(2)	4	252.9

Table 2. Crystallographic Data for $[\text{Mn}_{32}\text{Se}_{14}(\text{SePh})_{36}(\text{PnPr}_3)_4]$ (**1**) and $[\text{Na}(\text{benzene-15-Crown-5})(\text{C}_4\text{H}_8\text{O})_2]_2[\text{Mn}_8\text{Se}(\text{SePh})_{16}]$ (**2**)

	1	2 · 0.5 thf
<i>fw</i> [g/mol]	9122.59	3778.28
crystal system	cubic	monoclinic
space group	<i>P</i> 23	<i>P</i> 2 ₁ /c
Cell		
a [Å]	22.272(3)	29.265(6)
b		21.122(4)
c		26.029(5)
α [°]		
β		102.54(3)
γ		
<i>V</i> [Å ³]	11049(2)	15705(5)
<i>Z</i>	1	4
<i>T</i> [K]	160	180
<i>d_c</i> [g cm ⁻³]	1.371	1.598
<i>μ</i> (Mo-Kα) [mm ⁻¹]	6.789	4.617
<i>F</i> [000]	4336	7376
2θ _{max} [°]	49	49
meas reflns	15661	96176
unique reflns	4340	26314
<i>R</i> _{int}	0.1002	0.0692
reflns with <i>I</i> > 2σ(<i>I</i>)	3822	20496
refined params	240	1330
<i>R</i> 1(<i>I</i> > 2σ(<i>I</i>)) ^a	0.0524	0.0696
<i>wR</i> 2(all data) ^b	0.1392	0.2253
<i>Abs. Struct. Param.</i>	0.06(2)	

^a R1 = Σ||*F*_o| - |*F*_c||/Σ|*F*_o|. ^b wR2 = {Σ[w(*F*_o²-*F*_c²)²] / Σ[w(*F*_o²)²]}^{1/2}

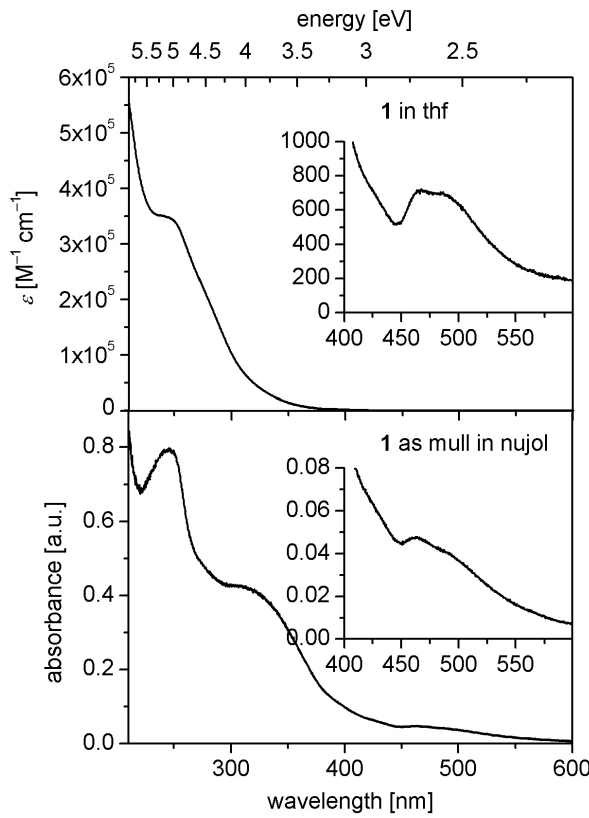


Figure 3. UV-Vis spectra of $[\text{Mn}_{32}\text{Se}_{14}(\text{SePh})_{36}(\text{PnPr}_3)_4]$ (**1**) in THF (top) and solid state (bottom).

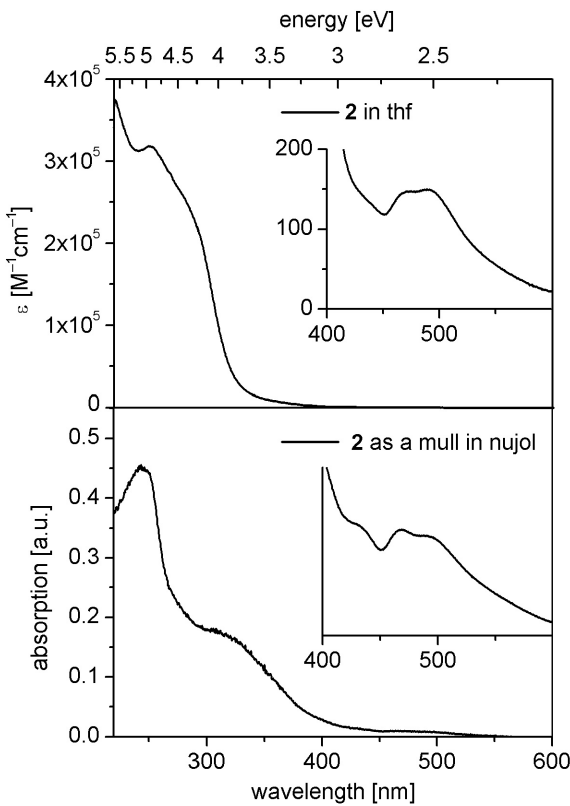


Figure 3. UV-Vis spectra of $[\text{Na}(\text{benzene-15-Crown-5})(\text{C}_4\text{H}_8\text{O})_2]_2[\text{Mn}_8\text{Se}(\text{SePh})_{16}]$ (**2**) in THF (top) and solid state (bottom).

References

- [1] A. Eichhöfer, R. Viswanath, P. Wood, *Eur. J. Inorg. Chem.* submitted.
- [2] N. Miyoshi, H. Ishii, K. Kondo, S. Mui, N. Sonoda, *Synthesis* **1979**, 301 – 304.
- [3] H. Schmidt, H. Ruf, *Z. Anorg. Allg. Chem.* **1963**, *321*, 270 – 273.
- [4] G. M. Sheldrick, SHELXTL PC version 5.1 An Integrated System for Solving, Refining, and Displaying Crystal Structures from Diffraction Data, Bruker Analytical X-ray Systems, Karlsruhe, 2000.
- [5] E. Keller, SCHAKAL 97, A Computer Program for the Graphic Representation of Molecular and Crystallographic Models, Universität Freiburg, 1997.
- [6] A.L. Spek, *Acta Cryst.* **1990**, *A46*, C-34.
- [7] STOE, WinXPOW, STOE & Cie GmbH, Darmstadt, 2000.
- [8] O. Kahn, *Molecular Magnetism*, Wiley-VCH, Weinheim, 1993